polymer

Viscoelastic characterization of moderately concentrated polystyrene solutions by dynamic light scattering

Yoshiyuki Einaga[a],*, Toyohiko Fujisawa[b]

[a]*Department of Chemistry, Nara Women's University, Nara 630-8506, Japan*
[b]*Department of Polymer Chemistry, Kyoto University, Kyoto 606-8501, Japan*

Abstract

The dynamic light scattering measurements were performed for moderately concentrated entangled solutions of atactic polystyrene in benzene (BZ) at 25.0 °C, in cyclohexane (CH) at 34.5 °C (Θ), and in diethyl malonate (DEM) at 35.0 °C (Θ) to characterize their viscoelastic properties. The results have shown that while the mutual diffusion coefficient D increases in the BZ solutions and decreases in the CH and DEM solutions with increasing polymer mass concentration c, the friction coefficient ζ for the three solutions increases with c showing the same power-law behavior irrespective of the weight-average molecular weight M_{w} and solvent quality. It has been found that the instantaneous longitudinal modulus L_0 for the CH and DEM solutions increases in proportion to c^2, obeying the familiar relation for the plateau value $(4/3)G_{\mathrm{N}}$ of the longitudinal stress relaxation modulus, but the L_0 values for these solutions are somewhat smaller than the values predicted from the relation. The terminal relaxation time τ_{m} for the two Θ solvent systems has been found to follow the power-law $\tau_{\mathrm{m}} \propto c^{2.7}$, showing good correspondence to the relation established by rheological measurements. © 2002 Elsevier Science Ltd. All rights reserved.

Keywords: Dynamic light scattering; Viscoelasticity; Polystyrene

1. Introduction

In the recent work [1–7], it has been established that the correlation of concentration fluctuations in moderately concentrated polymer solutions decays with time by two mechanisms, i.e. mutual diffusion of polymer and solvent molecules due to gradients of their chemical potentials, and viscoelastic relaxation of polymer chains due to the stress generated by disturbances of their equilibrium distributions. Thus, the dynamic light scattering (DLS) experiments, which yield the dynamic scattering factor $S(q,t)$ with q and t being the magnitude of scattering vector and time, respectively, affords a good means to determine viscoelastic properties of polymer solutions under rigorously controlled solvent conditions to which conventional rheological techniques are hardly accessible. In the previous papers [6,7], we have theoretically developed a procedure to evaluate the longitudinal rubbery plateau modulus L_0 and terminal relaxation time τ_{m} in addition to the mutual diffusion coefficient D and friction coefficient ζ of entangled

polymer solutions from $S(q,t)$. The method has been successively applied to moderately concentrated polyisobutylene solutions under the good and Θ conditions [7,8].

In the present work, we have studied solvent dependence of D, ζ, L_0, and τ_{m} as functions of polymer molecular weight and concentration for moderately concentrated solutions of atactic polystyrene (a-PS) in good and Θ solvents.

2. Experimental

2.1. Materials

The a-PS samples F128 and F288 used in this work are the standard samples supplied by Tosoh Co. Ltd. The values of their weight-average molecular weight M_{w} determined by static light scattering (SLS) in toluene at 15.0 °C are 1.18×10^6 for F128 and 3.13×10^6 for F288.

The solvents toluene used for SLS measurements and benzene (BZ), cyclohexane (CH), and diethyl malonate (DEM) used for DLS measurements were purified by distillation according to standard procedures prior to use.

---

* Corresponding author. Tel./fax: +81-0742-20-3400.
E-mail address: einaga@cc.nara-wu.ac.jp (Y. Einaga).

2.2. Static and dynamic light scattering

SLS measurements were carried out to determine M_w for the a-PS samples in toluene at 15.0 °C. A Fica 50 light scattering photometer was used for all the measurements with vertically polarized incident light of wavelength 436 nm.

DLS measurements were made to obtain the normalized autocorrelation function $g^{(2)}(t)$ for the BZ, CH, and DEM solutions, using a Brookhaven Instruments Model BI-200SM light scattering goniometer and vertically polarized incident light of 488 nm wavelength from a Spectra-Physics Model 2020 argon ion laser equipped with a Model 583 temperature-stabilized etalon for single-frequency mode operation. The photomultiplier tube used was an EMI 9863B/350, and the output was processed by a Brookhaven Instruments Model BI2030AT autocorrelator with 264 channels. The results for $g^{(2)}(t)$ were analyzed according to the same procedure as described in our previous papers [7,8] in order to determine D from the first cumulant K_1 of $g^{(1)}(t)$ and L_0 and τ_m from the spectrum analysis of $g^{(1)}(t)$. Here, use was made of the Siegert relation

$$g^{(2)}(t; \Delta t) = g^{(2)}(t) = 1 + f|g^{(1)}(t)|^2 \qquad (1)$$

with f being the constant determined by the optical system used. The electric field correlation function $g^{(1)}(t)$ is substantially the same as $S(q, t)$.

DLS measurements were made for the BZ solutions at 25.0 °C, for the CH solutions at 34.5 °C (Θ), and for the DEM solutions at 35.0 °C (Θ). For all the a-PS solutions, the polymer mass concentration c is in the range where polymer chains are moderately or highly entangled. Note that the value of the critical molecular weight M_c for the onset of entanglements is estimated as 3.12×10^4 for bulk a-PS [9]. To prepare the test solution, a dilute solution of the a-PS sample in benzene or cyclohexane was filtered into an optically cleaned light scattering cell with a Teflon membrane of 0.45 μm pore size. The solution was freeze-dried after the cell was covered with a Teflon membrane of the same pore size. Then, an appropriate amount of filtered solvent BZ, CH or DEM was poured into the cell. After the cell was tightly sealed, the solution was made homogeneous keeping the cell for 10–14 days at ca. 50 °C for CH and DEM, and at room temperature for BZ. The polymer mass concentration c was calculated from the weight fraction and the solution density.

3. Results and discussion

3.1. Solvent dependence of the autocorrelation function

Fig. 1 depicts examples of solvent dependence of the autocorrelation function $[g^{(2)}(t) - 1]^{1/2}$ for the sample F288 at $c \simeq 0.05$ g/cm^3 and at scattering angle $\theta = 60$ °. We find

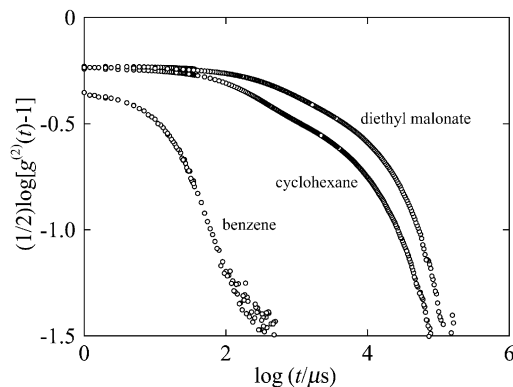

Fig. 1. Double-logarithmic plots of $[g^{(2)}(t) - 1]^{1/2}$ against t for the sample F288 in BZ, CH, and DEM at $c \simeq 0.05$ g/cm^3 and at the scattering angle $\theta = 60°$.

that the data set for each solution approximately consists of two components, i.e. fast and slow modes. For the two Θ solvent systems, i.e. the CH and DEM solutions, contributions of the slow modes to $[g^{(2)}(t) - 1]^{1/2}$ are considerably large; the magnitude of the slow modes is roughly comparable to that of the fast one. On the other hand, the magnitude of the slow mode is extremely small for the case of the BZ solution. The present results may be interpreted as follows. The fast mode is mainly due to the mutual diffusion of polymer and solvent molecules, and the slow one is mainly ascribed to the viscoelastic relaxation of entanglement network of polymer chains as discussed by Adam and Delsanti [1] and Štěpánek and Brown [10], although this separation of the mechanisms is not rigorous. Thus, the amplitude of the fast component is approximately determined by the osmotic modulus of the solution and the modulus strongly increases with solvent quality. This is the reason why contributions of the fast and slow modes to $[g^{(2)}(t) - 1]^{1/2}$ vary with solvent quality. As to the present results, we note that benzene is a very good solvent for a-PS.

Similar results as those shown in Fig. 1 were obtained at different scattering angles and also for all the solutions examined. In principle, it is difficult to analyze the results of $[g^{(2)}(t) - 1]^{1/2}$ over the entire range of time t for the solutions in a very good solvent. Thus, for the present case, the results for the BZ solutions were subjected only to the cumulant analysis in order to determine D and ζ, while viscoelastic properties were also extracted from $[g^{(2)}(t) - 1]^{1/2}$ for the Θ solvent systems in addition to these properties.

3.2. Mutual diffusion and friction coefficients

The mutual diffusion coefficient D was evaluated from the first cumulant K_1 according to the relation

$$K_1 = Dq^2 \qquad (2)$$

as described in previous papers [7,8]. In Fig. 2, the D values for the BZ (squares), CH (circles), and DEM (triangles)
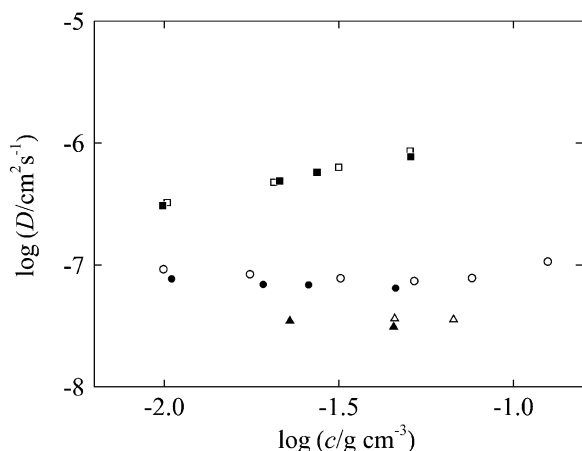
Fig. 2. Double-logarithmic plots of D against c for the samples F128 (unfilled symbols) and F288 (filled symbols) in BZ at 25.0 °C (squares), in CH at 34.5 °C (Θ) (circles), and in DEM at 35.0 °C (Θ) (triangles).

solutions are double-logarithmically plotted against c. It is seen that D of the BZ solutions increases with increasing c following a straight line, while those of the CH and DEM solutions follow curves slightly convex downward, as found previously for the polyisobutylene (PIB) solutions in good and Θ solvents [8]. We find that D for each solvent system is almost independent of polymer molecular weight.

From the values of D, the friction coefficient ζ was calculated by [11,12]

$$D = \frac{(1 - vc)^2}{\zeta}\left(\frac{\partial \pi}{\partial c}\right)_{T,p} \tag{3}$$

where v is the partial specific volume of the solute component, π the osmotic pressure, T the absolute temperature, and p the pressure. Here, we used the $(\partial \pi / \partial c)_{T,p}$ values calculated from

$$\left(\frac{\partial \pi}{\partial c}\right)_{T,p} = RT\left(M_w^{-1} + 2A_2 c + 3A_3 c^2\right) \tag{4}$$

with R being the gas constant and A_2 and A_3 the second and third virial coefficients, respectively. It is to be noted that although the use of Eq. (4) is an approximation, it gives good evaluation of $(\partial \pi / \partial c)_{T,p}$, since the present work is concerned with moderately concentrated solutions. In the present work, the literature values [13,14] of A_2 and A_3 were used for the BZ and CH solutions and those for the DEM solutions were set equal to zero. The values of ζ thus obtained are double-logarithmically plotted against c in Fig. 3. The results show that ζ increases with increasing c following straight lines with slope ca. 1.2 irrespective of the solvent species, although the data points for the DEM solutions are highly scattered. The value of the slope is substantially independent of M_w and solvent quality. This result implies that distinct difference in the c dependence of D between the good and Θ solvent systems found in Fig. 2 is attributed to the dependence of the driving force of the mutual diffusion, i.e. $(\partial \pi / \partial c)_{T,p}$, on the solvent quality.
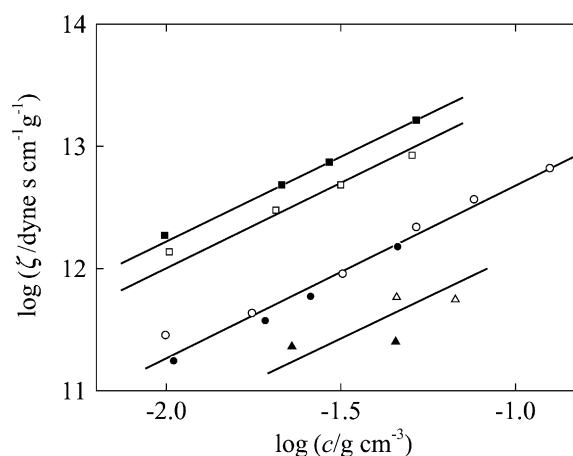

Fig. 3. Double-logarithmic plots of ζ against c for a-PS in BZ, CH, and DEM. The symbols have the same meaning as those in Fig. 2. The solid straight lines are drawn with a slope 1.2.

3.3. Rubbery plateau modulus

The values of the instantaneous longitudinal modulus L_0 for the CH and DEM solutions were determined from the discrete spectrum analysis of $[g^{(2)}(t) - 1]^{1/2}$ as described before. They are double-logarithmically plotted against c in Fig. 4 for the CH (circles) and DEM (triangles) solutions. According to the theoretical analysis by Chen and Berry [2], L_0 may be correlated to the rubbery plateau modulus G_N by

$$L_0 = (4/3)G_N \tag{5}$$

Thus for reference, Fig. 4 includes the value of $(4/3)G_N$ determined for bulk a-PS [15,16] (diamond) by mechanical or rheological measurements. The straight line in this figure represents the familiar relation [2,17]

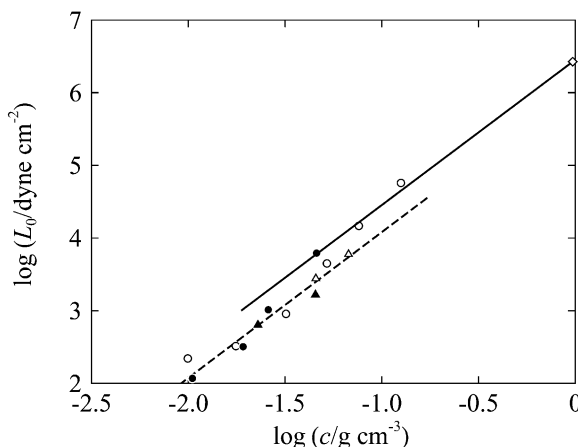$$G_N = G_N^0\left(\frac{c}{\rho^0}\right)^2 \tag{6}$$

Fig. 4. Double-logarithmic plots of L_0 against c for a-PS in CH and DEM. Diamond indicates the value for bulk a-PS. The other symbols have the same meaning as those in Fig. 2. The solid line represents the values calculated by Eq. (6). The dashed straight line is drawn with a slope 2.
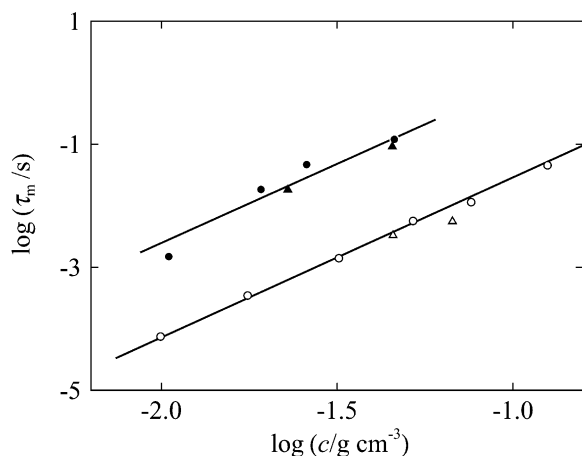
Fig. 5. Double-logarithmic plots of τ_m against c for a-PS in CH and DEM. The symbols have the same meaning as those in Fig. 2. The solid straight lines are drawn with a slope 2.7.

where G_N^0 is the rubbery plateau modulus and ρ^0 is the density of pure a-PS.

The L_0 values are approximately independent of M_w and solvent species. As to this point, we note that G_N^0 is known to be independent of M_w. We may represent the c dependence of L_0 as $L_0 \propto c^2$ as indicated by the dashed line in coincidence with Eq. (6). However, the present data are somewhat smaller than those expected from Eq. (6) except for the few data points at high concentrations, as in the case of the PIB solutions studied previously [8]. The behavior suggests that the entanglement density or the number of entanglements per unit volume decreases with decreasing c at Θ state.

3.4. Terminal relaxation time

Fig. 5 shows double-logarithmic plots of the terminal relaxation time τ_m against c for the CH (circles) and DEM (triangles) solutions. In the region of c observed, the τ_m vs c relation is found to obey a power-law behavior with the same exponent ca. 2.7 irrespective of M_w and solvent quality. At fixed c, the ratio of τ_m of two different M_w is in close agreement with the ratio of $M_w^{3.4}$. This result is in good coincidence with the familiar relation $\tau_m \propto M_w^{3.4}$ established for the entangled polymer systems by rheological measurements [9,17].

The c dependence of τ_m may be discussed by using the relation [17,18]

$$\tau_m = \zeta_s(c)F(c,M) \tag{7}$$

where $\zeta_s(c)$ is the segmental friction coefficient and the $F(c,M)$ is the structure factor due to the entanglement network which is represented as

$$F(c,M) \propto \frac{\eta_{if}(c,M)}{G_N(c)} \propto \frac{(cM)^{3.4}}{G_N(c)} \tag{8}$$

with $\eta_{if}(c,M)$ being the viscosity at iso-segmental-friction state. If we assume that the c dependence of $\zeta_s(c)$ is the same as that of ζ shown in Fig. 3, Eqs. (7) and (8) predict τ_m as a function of c as

$$\tau_m \propto c^{2.6} \tag{9}$$

since G_N is roughly proportional to c^2 as found in Fig. 4. The exponent in Eq. (9) is in close agreement with the present experimental observations given in Fig. 5. However, in the previous work [8], we have obtained different results for the PIB solutions; the observed exponents in τ_m as a function of c have been larger than the prediction by Eqs. (7) and (8), suggesting that the c dependence is different for ζ_s and ζ. Further work is definitely required to obtain clear conclusion on this problem.

Acknowledgments

References

[1] Adam M, Delsanti M. Macromolecules 1985;18:1760.
[2] Chen S-J, Berry GC. Polymer 1990;31:793.
[3] Doi M, Onuki A. J Phys II (Paris) 1992;2:1631.
[4] Onuki A. J Non-Cryst Solids 1994;172–174:1151.
[5] Berry GC. Adv Polym Sci 1994;114:233.
[6] Einaga Y, Fujita H. Polymer 1999;40:565.
[7] Einaga Y, Karube D. Polymer 1998;40:157.
[8] Einaga Y, Itaya A, Takaoka M. Polymer, in press.
[9] Ferry JD. Viscoelastic properties of polymers, 3rd ed. New York: Wiley; 1980.
[10] Štěpánek P, Brown W. Macromolecules 1998;31:1889.
[11] Berne BJ, Pecora R. Dynamic light scattering. New York: Wiley; 1976. Chapter 13.
[12] Štěpánek P, Brown W, Hvidt S. Macromolecules 1996;29:8888.
[13] Nakamura Y, Norisuye T, Teramoto A. Macromolecules 1991;24:4904.
[14] Nakamura Y, Norisuye T, Teramoto A. J Polym Sci, Part B: Polym Phys Ed 1991;29:153.
[15] Fetters LJ, Lohse DJ, Milner ST, Graessley WW. Macromolecules 1999;32:6847.
[16] Fetters LJ, Lohse DJ, Richter D, Witten TA, Zirkel A. Macromolecules 1994;27:4639.
[17] Einaga Y, Osaki K, Kurata M, Tamura M. Macromolecules 1972;5:635.
[18] Casassa EF, Berry GC. In: Allen G, editor. Comprehensive polymer science, vol. 2. New York: Pergamon Press; 1988. Chapter 3.